Int. J. Electrochem. Sci., 14 **(2019)** 2216 – 2223, doi: 10.20964/2019.03.02

International Journal of
ELECTROCHEMICAL
SCIENCE
www.electrochemsci.org

Short Communication

Effect of Flow Rate on Corrosion Behavior and Hydrogen Evolution Potential of X65 Steel in 3.5% NaCl Solution

Weiwei Kang, Zhiming Gao[*], *Yingjie Liu, Liqin Wang*

School of Material Science and Technology, Tianjin University, Tianjin, 30072, China
[*]E-mail: gaozhiming@tju.edu.cn

Received: 19 March 2017 / *Accepted:* 29 December 2018 / *Published:* 7 February 2019

Effect of flow rate on the cathodic reaction as well as hydrogen evolution potential of X65 steel in 3.5% NaCl solution were investigated using Electrochemical impedance spectroscopy (EIS) and potentiodynamic polarization. It is observed that, compared with static conditions, the charge transfer resistance values R_t decreases significantly under the condition of flowing, and the cathodic diffusion limiting current density increases with the increasing of the flow rate. In addition, the polarization curve under static conditions appears a typical hydrogen evolution potential turning point while the polarization curve under flowing condition does not. The determination of hydrogen evolution potential by means of measuring EIS under different cathodic potentials shows that the hydrogen evolution potential of X65 shifts positively to different degrees with the increasing of flow rate.

Keywords: flow rate; cathodic protection; hydrogen evolution potential; X65 steel.

1. INTRODUCTION

Cathodic protection is an extensively used method in marine engineering. It has made a great deal of mature theoretical basis after years of research and practice [1-4]. At present, hydrogen evolution potential is regarded as the minimum potential of cathodic protection, so hydrogen evolution potential is an important parameter for cathodic protection. Previous studies have shown that if the cathodic protection potential is negative than the hydrogen evolution potential, it may cause hydrogen embrittlement which will lead to a deterioration in mechanic performance of materials [5-9]. For example, when the cathodic protection potential applied for X65 steel reaches to -1200 mV (versus saturated calomel electrode), the region of brittle fracture will rise and hydrogen-induced embrittlement failures occur [10]. In addition, the effect of cathodic protection depends largely on the environment and the properties of materials especially in the environment which will produces high velocity, such as marine environment, power stations, oil and gas production systems [11-13]. The flow rate will have great influence on the behavior of cathodic protection [14]. The transport of oxygen

to the surface of a metal under cathodic polarization in seawater is important [15]. For the materials covered with coatings, with the increase of flow rate, the problem of coating degradation become more and more serious and the corrosion rate is growing [16]. However, previous works mainly focused on flow rate effects on the cathodic electrochemical behavior, limited investigations have been conducted focusing on the flow rate effects on the hydrogen evolution potential. Therefore, studies of effect of flow rate on the hydrogen evolution potential are relatively lack and urgently needed to explore. In this work, X65 steel is used for research. We mainly discuss the effect of flow on the cathodic reaction and whether it will affect the hydrogen evolution potential.

2. EXPERIMENTAL

2.1 Materials and Preparation

The material used for research is X65 steel, and its chemical composition is shown in Table 1. A specimen of 10×10 mm in side length and 2 mm in thickness was used. The specimens were connected to a copper wire at one side to provide electrical contact and then embedded in epoxy resin, with the working area of 1 cm^2. The surface of the specimens were abraded with carbide paper (from 100# to 1500#) then washed by distilled water, degreased by ethanol and dried by cool air. The experiment medium was 3.5% NaCl solution. Experiments were carried out at 2 m/s, 4 m/s and 6 m/s, respectively. All the experiments were performed with a self-made recycling jet device at the room temperature.

Table 1 Chemical composition (wt. %) of X65 steel

C	Mn	Si	Cr	P	S	Ni	Cu	Mo
0.05	1.51	0.23	≤0.25	≤0.02	≤0.04	≤0.30	≤0.30	≤0.30

2.2 Polarization Curve Measurement

The potentiodynamic polarization curves were measured by the PARSTAT 2273 electrochemical system. A three-electrode configuration was used for the experiment. The specimen was the working electrode, platinum sheet was the counter electrode and a saturated calomel electrode (SCE) with a salt bridge was the reference electrode. The cathodic polarization curves of X65 steel in different flow rate were performed from open circuit potential (OCP) to-0.60 V (VS.OCP) at a scan rate of 0.166 mV/s.

2.3 Electrochemical Impedance Spectroscopy Measurement

The electrochemical impedance spectroscopy tests were also carried out by PARSTAT 2273 system. A three-electrode system the same as the cathodic polarization curve test was used for the experiment. The test parameters were set to sine wave voltage amplitude for 10 mV and scan

frequency range were 100 KHZ-10 MHZ. The test started from the open circuit potential and then negative shift of 50 mV of cathodic protection potential one after another. Each constant potential should be pre-polarized for 10 minutes before the EIS test. What is more, each test was repeated three times to ensure the accuracy of data. At last, with selected proper equivalent circuit, the test data was fitted and analyzed by the Zsimpwin software to get the electrochemical parameters, such as charge transfer resistance R_t and so on.

3. RESULTS AND DISCUSSION

3.1 Polarization curve Measurements

The cathodic polarization curves of X65 steel at different flow rates are shown in Fig.1. Compared with the static conditions, there is a significant increase of limiting diffusion current density under the flowing conditions, from 4.217×10^{-5} A·cm^{-2} increases to 1.26×10^{-3}A·cm^{-2}. It also has a small increase with the increasing of flow rate under flowing conditions. The values of limiting diffusion current density are shown in table 2. In addition, Fig.3 shows that the maximum of R_t has a great decrease under flowing conditions compare to that under static conditions, from 55200 Ω·cm^2 reduces to 628.70 Ω·cm^2 which can be seen in R_t-E curves. Above phenomena indicate that with the increasing of the flow rate, the corrosion rate of X65 steel accelerates. This phenomenon is consistent with previous studies of other steels, which also shows that the increase of the flow rate weakens the effect of cathodic protection and increases the density of protective current [17, 18].

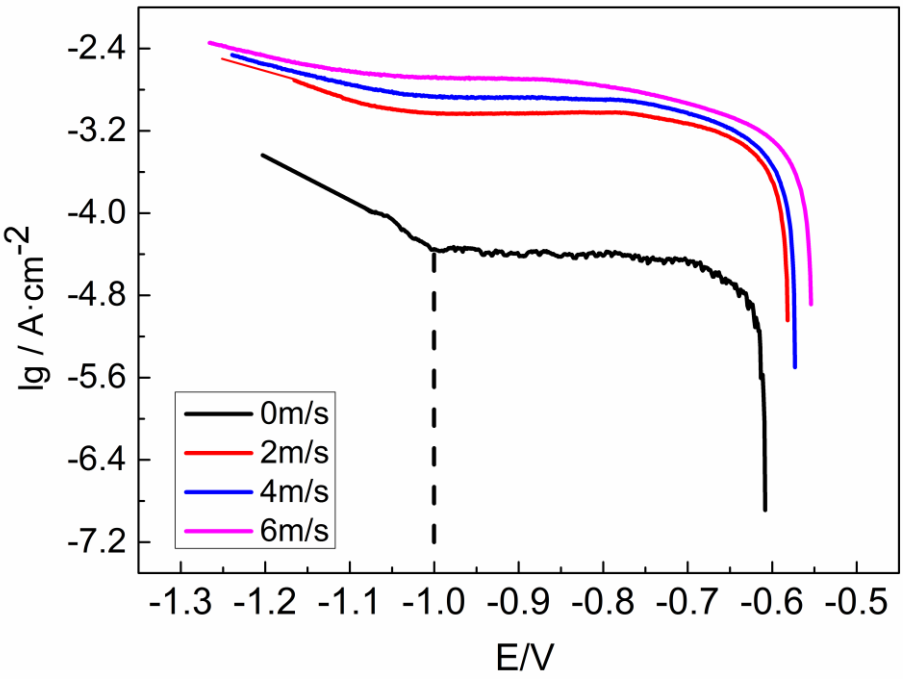

Figure 1. Polarization curves measured at different flow rates [0 m/s (black), 2 m/s(red), 4 m/s(blue), 6 m/s(pink)]

As we can see from the Fig.1, the cathodic polarization curve of X65 steel has the typical characteristics under static condition. The hydrogen evolution potential turning point is obvious, which is about -1.00 V_{SCE}. However, the hydrogen evolution potential is not particularly obvious at three kinds of flow rate. It is difficult to determine the hydrogen evolution potential based on the polarization curve. Therefore, we need to obtain the hydrogen evolution potential at different flow rates by EIS [19].

Table 2. Limiting diffusion current density at different flow rates

Flow rate (m/s)	0	2	4	6
Current density(A·cm^{-2})	4.217×10^{-5}	1.26×10^{-3}	1.32×10^{-3}	2.05×10^{-3}

3.2 Electrochemical Impedance Spectroscopy Measurements

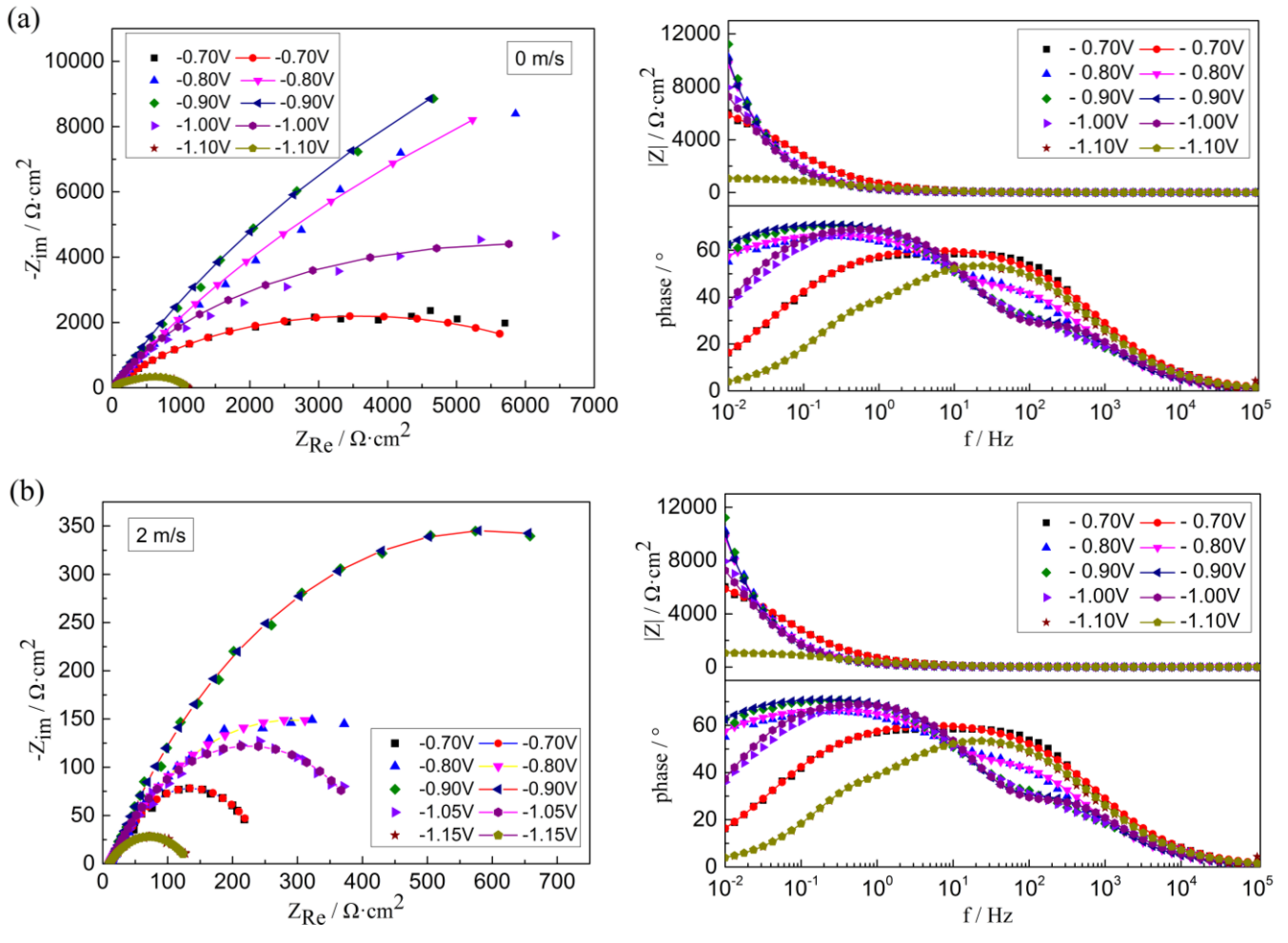

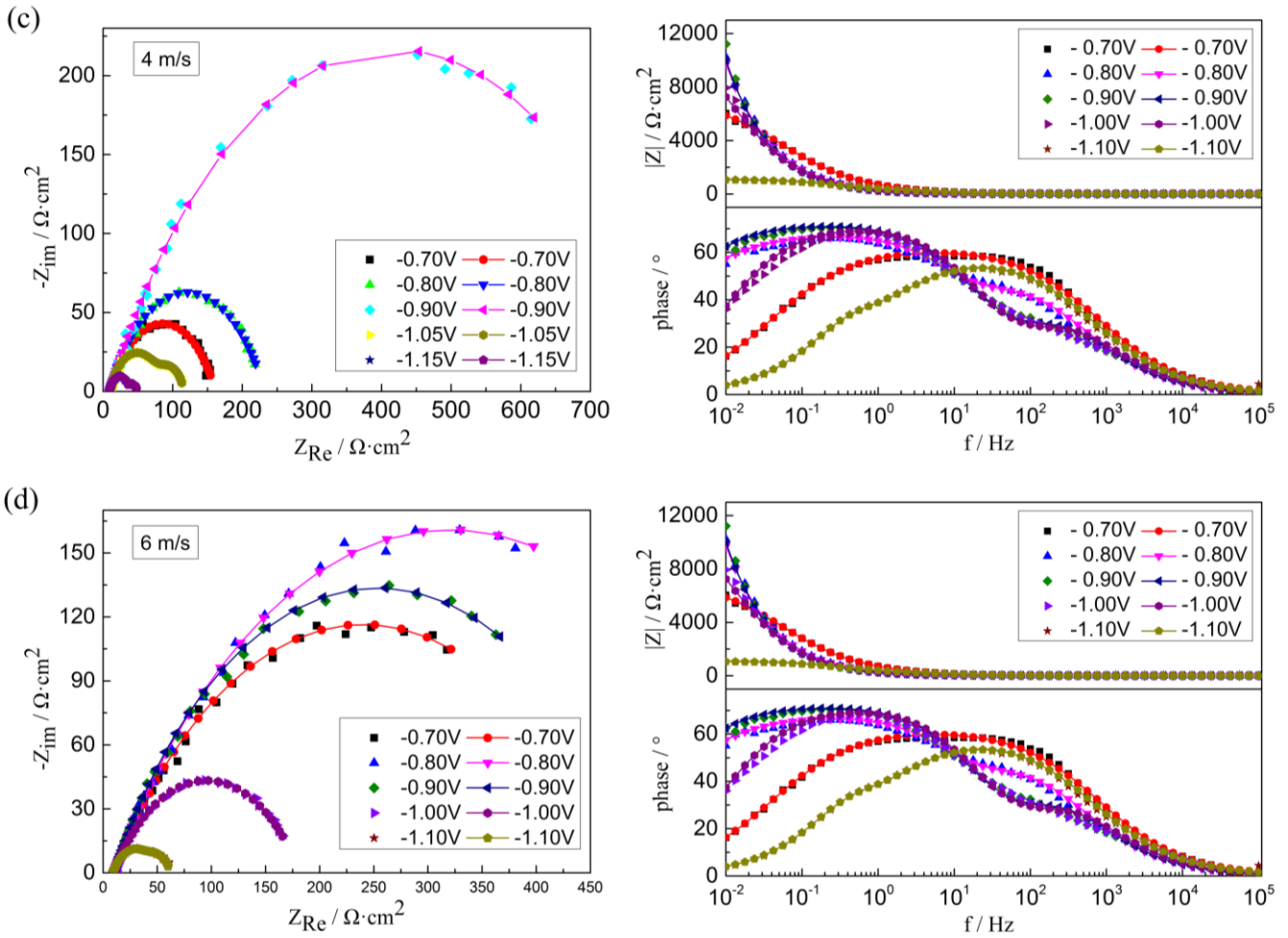

Figure 2. Electrochemical Impedance Spectroscopy measured at the flow rate of 0m/s (a), 2m/s (b), 4m/s (c) and 6m/s (d).

Fig.2 shows the experimental and fitting results of EIS of X65 steel at different flow rates in 3.5% NaCl solution (some typical results are given). It can be seen from the Fig.3, with the cathodic polarization potential shifts negatively, capacitive impedance loops all present a first increases and then decreases trend under different conditions. It shows that the corrosion process is controlled by cathodic reaction. In addition, one time constant can be inferred from the bode diagrams and the equivalent circuit was selected as $R(QR)$. In Fig.2, the point diagrams are the experimental results, and diagrams with points and lines mean the fitting results. Fig.2 shows that the fitting curves have a good match with the experimental results. The curves of the charge transfer resistance R_t as a function of cathode potential E are shown in Fig.3.

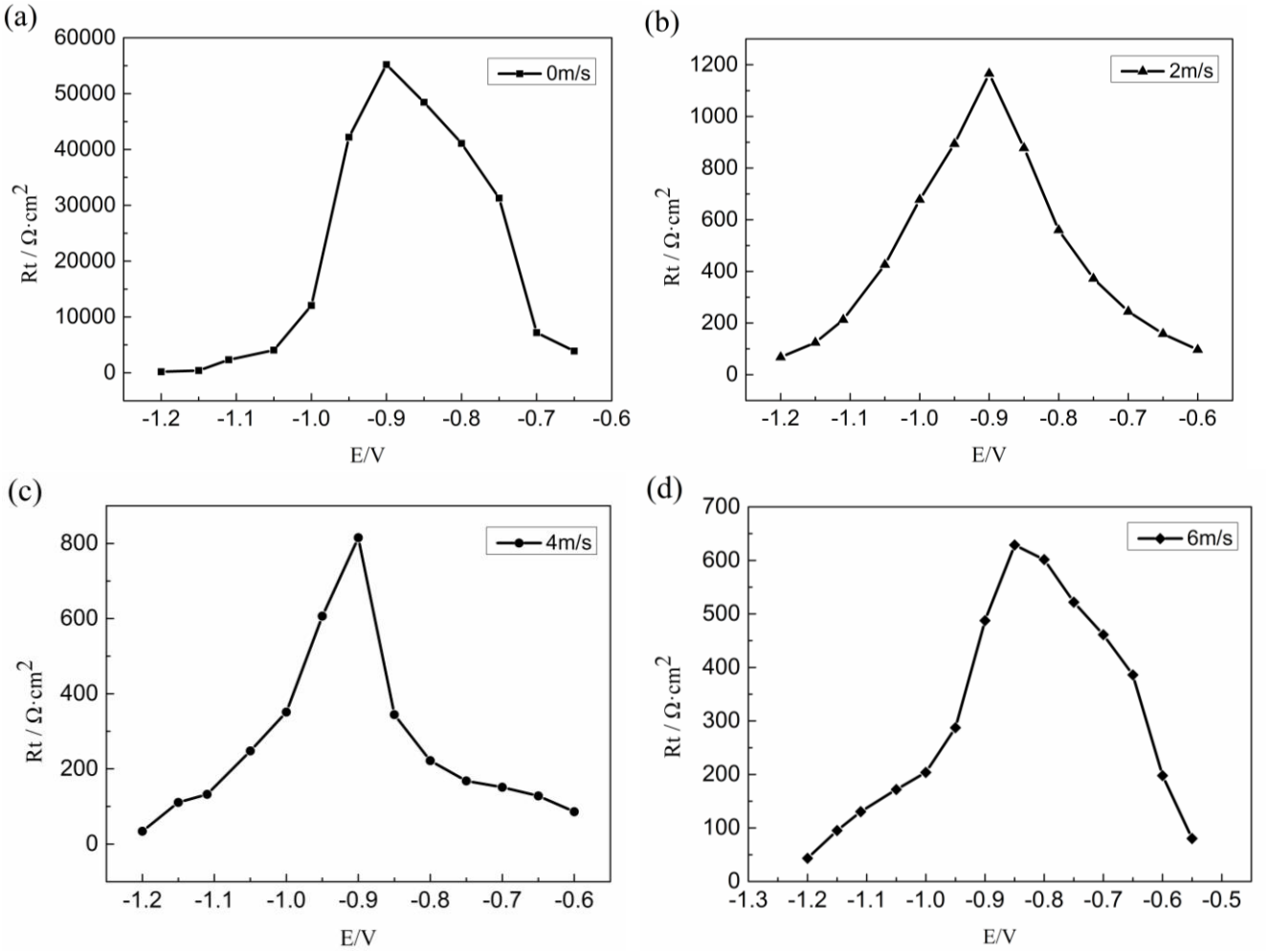

Figure 3. The trend of R_t as a function of E at the flow rates of 0m/s (a), 2m/s (b), 4m/s (c) and 6m/s (d).

According to the relevant theory [20, 21], the surface of X65 steel occur two kinds (anodic and cathodic reaction) of reactions simultaneously. Therefore, the EIS measured in cathodic polarization potential is the comprehensive response to the anodic and cathodic reaction. Thus the expression of charge transfer resistance of the impedance at the mixed potentials can be written as follows:

$$1/R_t = 1/Rt_a + 1/Rt_c$$

Where R_{ta} is the transfer resistance of anodic reaction and Rt_c is the transfer resistance of cathodic reactions. When applying cathodic polarization potential to the X65 steel, the anodic reaction will be suppressed, so R_{ta} increases with the potential negatively shifting. While R_{tc} reduces as a result of the cathode reaction performs more easily. When R_{ta} is much larger than R_{tc}, cathode reaction is the main reaction which occurred on the electrode surface.

When the cathodic polarization potential moved to a certain negative potential, except for the oxygen reduction reaction, the hydrogen evolution reaction also occurs. The expression of charge transfer resistance R_{tc} can be written as follows:

$$1/R_{tc} = 1/Rt_o + 1/Rt_H$$

Where Rt_o is the transfer resistance of oxygen reduction reaction and Rt_H is the transfer resistance of hydrogen evolution reaction. When the cathodic polarization potential just reaches the critical potential of hydrogen evolution reaction, it has a weak impact on the whole system, so Rt_H can be considered to be infinite, so Rt_c is approximately equal to Rt_o. But with the electrode potential becoming negative, Rt_c will decrease. When hydrogen reaction is obvious, Rt_H will become smaller and smaller as well as has an effect on Rt_c together with Rt_o. The decline of Rt_H would account for the decline of Rt_c, when the potential loss to a certain value, there will have a turning point in the R_t~E curve. The cathode potential of the turning point is considered to be the hydrogen evolution potential. The hydrogen evolution potentials obtained by the Rt~E curves are shown in Table.3.

Table 3. Hydrogen evolution potential obtained by electrochemical impedance spectroscopy measurement

Flow rate (m/s)	0	2	4	6
Hydrogen evolution potential (V)	-1.05~-1.00	-1.05~-1.00	-1.00~-0.95	-0.95~-0.90

Under the static conditions, according to the cathodic polarization curves in Fig.1, the hydrogen evolution potential of X65 steel in 3.5% NaCl solution is about -1.00 V_{SCE}. It is similar with that obtained by EIS, which is shown in Table.3. However, the hydrogen evolution potential at a flow rate of 2 m/s, 4 m/s and 6 m/s is -1.05~-1.00 V_{SCE}, -1.00~-0.95 V and -0.95~-0.90 V_{SCE} respectively. It shows that with the increase of flow rate, the hydrogen evolution potential of X65 steel shifts positively to different degrees. This phenomenon can be explained by the following reason. It is known that the hydrogen evolution reaction has three steps [22-24], where hydrogen ion becomes hydrogen atom and comes together as a hydrogen molecule is the determining step of the hydrogen evolution reaction dynamic behaviors. Because the existence of flow rate will promote the diffusion of hydrogen molecule from the metal surface to solution, the concentration of the hydrogen molecule on the electrode will be reduced, and accordingly the hydrogen partial pressure decreases. Therefore, the potential that hydrogen atom comes together to a hydrogen molecule requires will reduce, which means polarization potential shift less positively to maintain it. The greater the flow rate, the more obvious the trend. From this phenomenon, we can infer that if the same protection potential as static condition is also applied at high flow rate, the risk of hydrogen embrittlement will rise. Therefore, it is necessary to reduce the protection potential to avoid hydrogen embrittlement occurring at high flow rate.

4. CONCLUSIONS

(1) The flow velocity has a great influence on the cathodic reaction. With the increase of flow velocity, the charge transfer resistance decreases and the cathode current density increases, and the corrosion rate of X65 steel is accelerated. The corrosion potential increases with the flow rate.

(2) The flow rate also effects the hydrogen evolution potential. With the increasing of the flow rate, the hydrogen evolution potential of X65 steel shifts positively to different degrees.

(3) If the same protection potential as static condition is also applied at high flow rate, the risk of hydrogen embrittlement will rise. Therefore, It is necessary to reduce the protection potential to avoid hydrogen embrittlement occurring at high flow rate.

ACKNOWLEDGEMENTS
This research is supported by National Natural Science Foundation of China (No.51371124, No.51671144,), the Supporting Plan Project of Tianjin City (16YFZCGX00100) and Natural Science Foundation of Tianjin (No. 17JCTPJC47100).

References

1. L. Bertolini, F. Bolzoni, P. Pedeferri, L. Lazzari and T. Pastore, *J. Appl. Electrochem*., 28 (1998) 1321.
2. S. Eliassen, *Corros.Eng.Sci.Techn.*, 39(2004) 31.
3. C.F. Dong, A.Q. Fu, X.G. Li and Y.F. Cheng, *Electrochim. Acta*, 54 (2008) 628.
4. Z.Y. Liu, X.G. Li, C.W. Du, L. Lu and Y.R. Zhang, *Corros. Sci.*, 51 (2009) 2242.
5. M. Javidi and S. BahalaouHoreh, *Corros.Sci.*, 80 (2014) 213.
6. Seong-Jong Kim, Seok-Ki Jang and Jeong-Il Kim, *Met. Mater. Int.*, 11 (2005) 69.
7. Z.M. Gao, X.B. Lu, D.H. Xia, L.X. Yang, R.K. Zhu and Y. Behnamian, *Electrochemistry*, 84 (2016) 585.
8. D.G. Enos, A.J. Williams and J.R. Scully, *Corrosion*, 53 (1997) 891.
9. S.J. Kim, S.K. Jang and J.I. Kim, *Met. Mater. Int.*,11 (2005) 63.
10. T.M. Zhang and W.M. Zhao, *J. Chin. Soci. Corros. Prot.*, 34 (2014) 315.
11. S. Martinez, *Mater. Chem. Phys.*, 77 (2003) 97.
12. J. Konys, W. Krauss, H. Steiner, J. Novotny and A. Skrypnik, *J. Nucl. Mater.*, 417 (2011) 1191.
13. D.K. Kim and S. Muralidharan, *Electrochim. Acta*, 51 (2006) 5259.
14. T. Hong, Y.H. Sun and W.P. Jepson, *Corros. Sci.*, 44 (2002) 101.
15. S.W. Smith, K.M. McCabe and D.W. Black, *Corrosion*, 45 (1989) 790.
16. M. Ferry and W.B. Nik, *Mech. Mater. Eng.*, 55 (2014) 218.
17. F.Q. Fan, J.W. Song, C.J. Li and M. Du, *J. Chin. Soci. Corros. Prot.*, 34 (2014) 550.
18. X. Tang, J. Wang and Y. Li, *Marine Sci.*, 29 (2005) 26.
19. Z.M. Gao, X.Y. Liu, L.J. Wen and W.W. Kang, *Int. J. Electrochem. Sci.*, 11 (2016) 3007.
20. J.J. M. Jebaraj, D.J. Morrison and I.I. Suni, *Corros. Sci.*, 80 (2014) 517.
21. C.N. Cao, Corrosion Electrochemistry Principles, Chemical Industry Press, (2008) Beijing, China.
22. W.Y. Chu, Hydrogen embrittlement and stress corrosion cracking, science press, (2013) Beijing, China.
23. D.H. Xia, S.B. Wu, Y. Zhu, Z.Q. Wang, Y.H. Sun, R.K. Zhu and J.L. Luo, *Electrochemistry*, 84 (2016) 238.
24. D.H. Xia, Y. Song, S. Song, S. Wu and C. Ma, *J. Tianjin Univ. (sci. tech.)*, (2018) accepted for publication. DOI:10.11784/tdxbz201711023.